Desalination and Water Treatment
www.deswater.com

doi: 10.5004/dwt.2022.28334

255 (2022) 136–144
April

Al_2O_3@SiO_2-chitosan synthesis via sol–gel process and its application for ciprofloxacin adsorption

Nacer Ferrah[a,b,*], Djamila Merghache[c], Ghizlane Lebar[b]

[a]*University Center of Naâma, BP 66, Naâma 45000 DZA, Algeria, Tel. +213 559310187; email: ferrahnacer@yahoo.fr/ nacer.ferrah@cuniv-naama.dz/daniella755@yahoo.fr*

[b]*Laboratory of Inorganic Chemistry and Environment, Department of Chemistry, Tlemcen University, Box 119, Tlemcen, Algeria*

[c]*Antibiotics, Antifungal, Physico-Chemistry, Synthesis and Biological Activity Laboratory, Department of Biology, Faculty of Natural Sciences and Life Sciences of the Earth and the Universe, University of Tlemcen, Algeria*

Received 28 July 2021; Accepted 13 February 2022

ABSTRACT

This study aims to investigate the solid-phase extraction procedure of the most prescribed antibiotics in the world, ciprofloxacin, by using aluminosilicates grafted chitosan (Al_2O_3@SiO_2-chitosan). The green adsorbent was synthesis via sol–gel process, and cross-linking with chitosan, in the presence of glutaraldehyde as chelating agent. The results show that the extraction yield of ciprofloxacin removal decreases in acidic medium, more than 52% of adsorption yield was obtained with an optimal pH solution of 5.77. The kinetic study shows also that ciprofloxacin adsorption was very fast at the initial stage of contact time up to 30 min when the equilibrium adsorption was established. The maximal adsorption capacity was found to be 31 mg g^{-1}, under optimum conditions. Ciprofloxacin uptake process followed the pseudo-second-order rate expression. Equilibrium isotherm for ciprofloxacin has been modeled successfully using Langmuir isotherm model. Thermodynamics study leads to a spontaneous and exothermic process for ciprofloxacin adsorption by Al_2O_3@SiO_2-chitosan (ΔH = –08.49 kJ mol^{-1}).

Keywords: Adsorption; Al_2O_3@SiO_2-chitosan; Sol–gel process; Ciprofloxacin; Kinetic and equilibrium study

1. Introduction

The environmental impact of trace pharmaceuticals was first brought to public attention in the 1990s, when pharmaceutical residues were discovered in drinking water in Europe [1–3]. Several studies show that more than 55 pharmaceuticals used are present in significant concentrations. Around 35 pharmaceuticals are found in concentrations up to 1,200 ng L^{-1} [4–6]. They are used for various applications, including anti-cancers, antibiotics, anti-inflammatory, anxiolytic, etc. and are particularly concentrated in hospital sewage [7,8]. The detection of pharmaceuticals in the environment and the analysis of their potential impacts to the human health and ecosystems have become relevant and emerging research subjects in order to find solutions and closing this emerging problem [9,10]. The contamination of environments by antibiotics, contributes to the development of antibiotic resistance and promotes transmission to humans [11].

Wastewater treatment systems (WWTS) are not specifically designed for the removal of pharmaceuticals, and the concentration of some of these pollutants in water remains high even after treatment with the conventional methods [12,13]. Sewage water treatment employ biological and physical processes, which are less efficient to remove these residues, and the pharmaceutical contaminants can still exist in treated water. Adsorption is an alternative low-cost, easy process, ecofriendly technology and it is based on the

* Corresponding author.

Presented at the International Virtual Conference on Water and Energy (ICWE 21), Hassiba Benbouali University of Chlef, Algeria, 25–27 May 2021

interaction of the pollutant with the adsorbent material. Different types of adsorbents interact with dyes, heavy metals and other organic substances and could achieve higher removal rates for pharmaceuticals than other conventional process [14–17]. Sol–gel process can offer the possibility for adsorbent preparation with specific surface characteristics (specific surface, pore size distribution, surface area, size of pores, etc.), in the aim that surface adsorbent can be more compatible and adequate for chemical structure of adsorbed substance.

The aim of this study is to investigate the adsorption of ciprofloxacin with a hybrid material Al_2O_3@SiO_2-chitosan, synthesis via sol–gel process. Chitosan was cross-linking Al_2O_3@SiO_2 as chelating agent. This adsorbent was examined for ciprofloxacin adsorption in the batch process. The effects of analytical parameters, like mercury ion concentration, pH and contact time was reported. Eventually a kinetic, diffusion and thermodynamic studies were also carried.

2. Experimental

2.1. Reagents

All chemical reagents used in this work were of analytical grade. Aluminum nitrate hexahydrate ($Al(NO_3)_3{\cdot}6H_2O$; 97%), ethanol (99%), acetic acid (99%), and tetraethoxysilane (TEOS) were purchased from Sigma-Aldrich. Chitosan (D-glucosamine), and glutaraldehyde were purchased from Merck. Hydrochloric acid, polyethylene glycol (PEG), ammonia (36%), sodium hydroxide and ciprofloxacin (98%) were obtained from Sigma-Aldrich. Ultrapure water was used throughout the work. Stock and standard solutions of ciprofloxacin were prepared by dissolving an appropriate amount of product in ultrapure water. Solutions of lower concentrations were prepared by the dilution of stock solution.

2.2. Apparatus

Fourier-transform infrared spectroscopy (FTIR) characterization was taken in Spectrum Two PerkinElmer model. KBr sample pellets were prepared by mixing sample and potassium bromide in a 1:75 ratio, pressing at 10 bar on a hydraulic press. The X-ray patterns of the adsorbent material was carried out using Rigaku MiniFlex 600 spectrometer in the 2θ range from 2.0° to 80.0° at a step of 0.020°, with CuKα radiations (λ = 1.5418 Å). UV-Visible spectra were measured using PerkinElmer Lambda 25 UV-Vis spectrophotometer. pH measurements for all solutions were taken on a potentiometer Adwa AD1030 with a combined glass electrode.

2.3. Synthesis and preparation of Al_2O_3@SiO_2-chitosan

The hybrid material Al_2O_3@SiO_2-chitosan was prepared by sol–gel method in the molar ratio of Al_2O_3@SiO_2 (9:1), respectively. Firstly, a mixture of $Al(NO_3)_3{\cdot}6H_2O$ (0.18 moles), 50.0 mL of ultrapure water, 5.0 mL of HNO_3 was stirred vigorously in a quartz reactor under reflux conditions ($T°$ = 70°C). In other hand, TEOS (0.10 moles) was dissolved in 30.0 mL of ethanol, and kept stirred for 60 min, at room temperature. After that, TEOS solutions was added drop by drop in the quartz reactor containing aluminium nitrate. 10.0 mL of ammonia solution (5%), was then added to the reactional solution, and kept all the night in the quartz reactor at room temperature for gelation. Then, the wet gel was washed several times with ultrapure water and ethanol. The obtained xerogel was dried and calcined at 200°C for 24 h. Al_2O_3@SiO_2 powder was dissolved again in ultrapure water, with 20, 0 mL of glutaraldehyde as cross-linking agent. Then, an homogenous chitosan solution (1.0 g of chitosan; 50 mL of H_2O; 5.0 mL acetic acid), was added to the mixture, and the reactional solution was kept for 4 h under room temperature. Finally, the hybrid material Al_2O_3@SiO_2-chitosan (Fig. 1) was washed several times with ultrapure water and ethanol for ciprofloxacin adsorption and removal.

2.4. Adsorption studies of ciprofloxacin onto Al_2O_3@SiO_2-chitosan

The adsorption of ciprofloxacin has been investigated in solid-phase extraction from aqueous medium, in a batch process. 0.010 g of Al_2O_3@SiO_2-chitosan was added to 30 mL of ciprofloxacin solution in a glass flask. The mixture was stirred at the appropriate time, necessary for adsorption equilibrium. The ciprofloxacin concentrations in the aqueous solution were determined, before and after adsorption, spectrophotometrically using UV-Vis spectroscopy. The adsorption yield (%) was determined using the following equation:

$$\text{Adsorption yield}(\%) = \left(\frac{C_0 - C_e}{C_0}\right)100\% \quad (1)$$

The adsorption capacity of ciprofloxacin onto Al_2O_3@SiO_2-chitosan, q_t (mg g^{-1}), was calculated by the following equation:

$$q_t\,(\text{mg/g}) = (C_0 - C_t)\cdot V \cdot \frac{M}{W} \quad (2)$$

where C_0, C_t and C_e, are the initial, time and the equilibrium concentrations of ciprofloxacin (mg L^{-1}). V is the volume of aqueous phase, W is the weight of the material adsorbent, and M is the atomic weight of ciprofloxacin. The effect of contact time in ciprofloxacin adsorption was studied until 180 min, for initial Hg(II) concentration of 20.0 mg L^{-1}. To investigate the effect of ciprofloxacin concentration, 0.01 g of Al_2O_3@SiO_2-chitosan was mixed with various concentrations of ciprofloxacin, ranging from 10.0 to 100.0 mg L^{-1} for 180 min until equilibrium state reached. The effect of initial pH solution on ciprofloxacin removal was studied by varying pH in the range from 1.0 to 9.0 at room temperature. Along with the parameter effects described above, ionic strength, and temperature effects were also reported in this work.

3. Results and discussion

3.1. FTIR analysis of Al_2O_3@SiO_2-chitosan

Fig. 2 shows the infrared spectrum for Al_2O_3@SiO_2-chitosan adsorbent before (a) and after (b) ciprofloxacin adsorption.

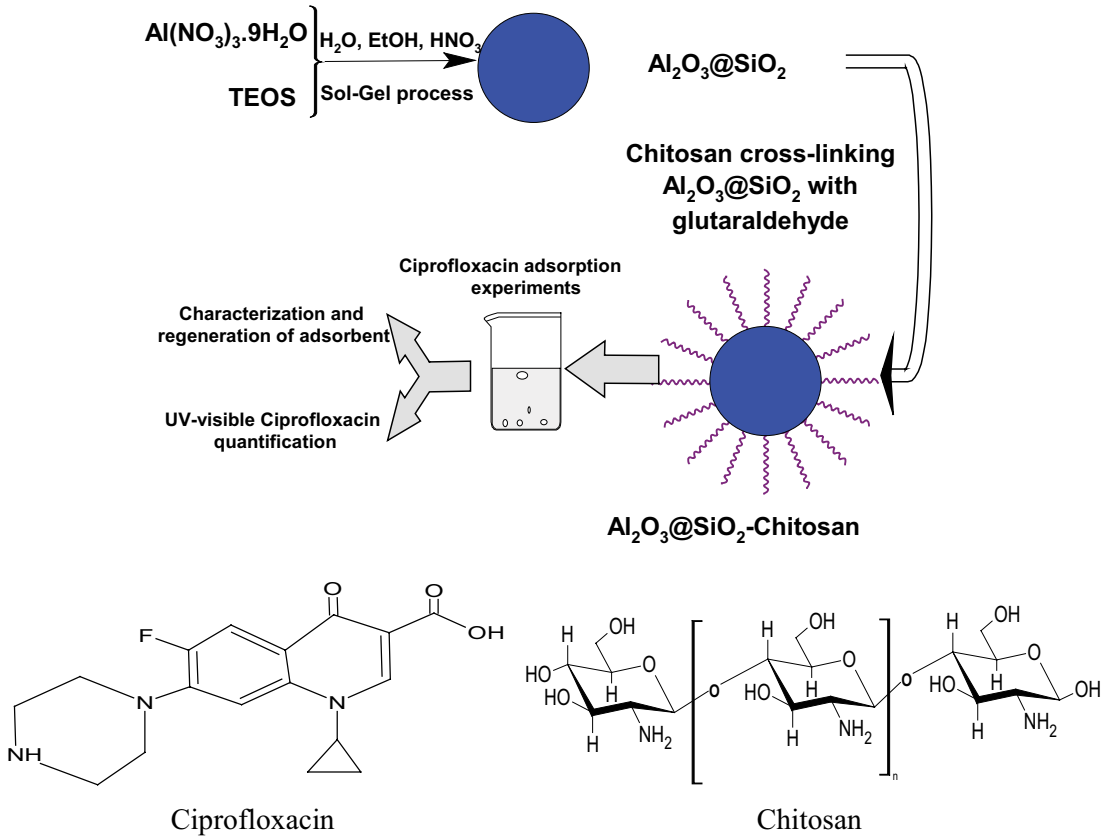

Fig. 1. Sol–gel process synthesis way of Al_2O_3@SiO_2-chitosan adsorbent.

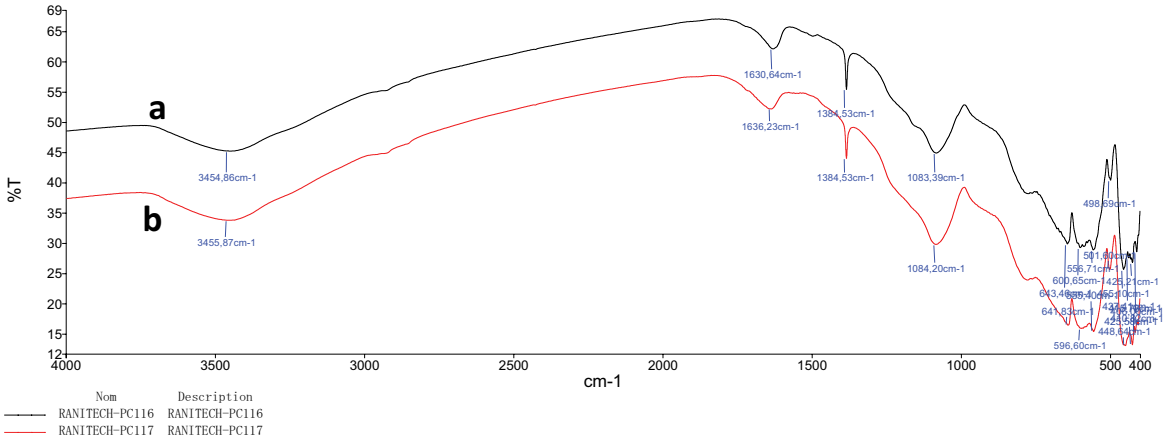

Fig. 2. FTIR spectra of Al_2O_3@SiO_2-chitosan before (a) and after (b) ciprofloxacin adsorption.

The peak at 596, 641 and 751 cm^{-1} can be attributed to the Al-O vibrations. The peaks from 400 to 448 cm^{-1} explains Si-O stretching vibration [18]. The bands at 1083 cm^{-1} correspond to H-N-H deformation vibration. A large peak was observed near 1636 cm^{-1} assigned to υ (-CO) stretching in carboxylate groups on chitosan matrix. The peak at 1384 represents the characteristic stretching vibration of glucosamine ring in chitosan polymer [19].

All these peaks prove that chitosan was successfully grafted onto Al_2O_3@SiO_2 surface with glutaraldehyde. The FTIR spectrum after ciprofloxacin adsorption indicates the same peaks and bands of Al_2O_3@SiO_2-chitosan with a slight shift, suggesting that ciprofloxacin has been well attached to the surface of adsorbent.

3.2. *X-ray diffraction analysis of Al_2O_3@SiO_2-chitosan*

Fig. 3 depicts the powder X-ray diffraction patterns of the Al_2O_3@SiO_2-chitosan adsorbent. The diffractograms of the adsorbent show similar and typical looks of crystalline

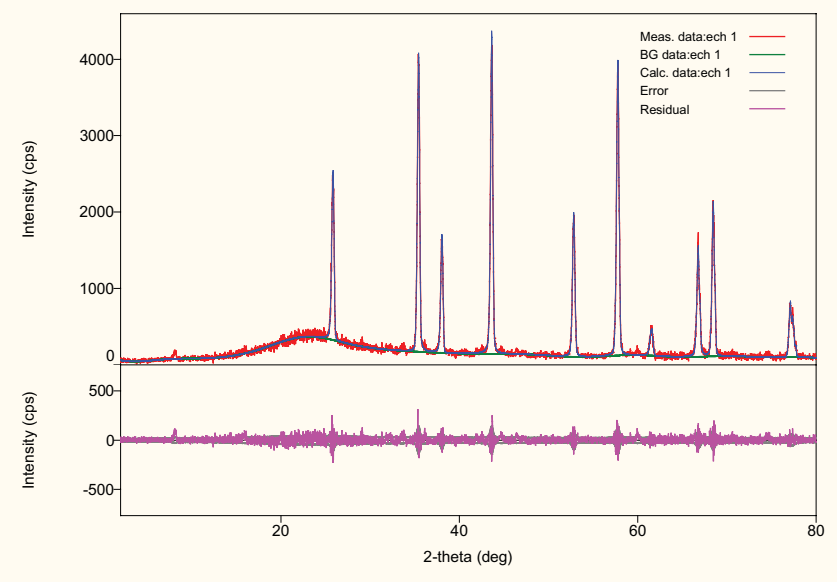

Fig. 3. X-ray diffraction patterns of the Al_2O_3@SiO_2-chitosan adsorbent.

materials. We note the presence of the first peak at 25.83 (100) corresponds to the SiO_2 phase [18]. The crystals of Al_2O_3 consist of monoclinic and cubic matrix. The peaks at 35.43 (104), 38.05 (110), 43.63 (113), and 68.47 (300) were attributed to the Al_2O_3 crystalline phase. The estimation of the crystalline particle size was calculated by the Debye-Sherer formula and the mean average size was found to be 54 nm. No changes in the diffraction patterns are observed of the cross-linking chitosan, and this result confirms that chitosan structure was grafted only onto the solid surface without changing the crystalline structure of Al_2O_3@SiO_2 [20].

3.3. Morphology and textural analysis of Al_2O_3@SiO_2-chitosan

The results of Al_2O_3@SiO_2-chitosan microstructure analysis investigated by scanning electronic microscopy (SEM), before and after ciprofloxacin adsorption are shown in Fig. 4. From SEM micrographs, it can be seen clearly the presence of different irregular and spherical aggregates, which are mostly agglomerated from a small crystal size around 1 μm to large crystal size around 20 μm [21]. After ciprofloxacin adsorption, the pores are less visible and the SEM micrograph indicates more graininess and smooth surface, with a layered structure. We suggest that the available surface was well saturated with ciprofloxacin molecules [22].

3.4. Effect of pH solution on ciprofloxacin adsorption

The pH solution is an important parameter influencing the ciprofloxacin adsorption, because the later has two acid dissociation constants (pKa), 2.5 and 8.7 respectively. Ciprofloxacin presents a cationic structure (pH < 2.5), zwitterionic forms (2.5 < pH < 8.8), or anionic forms (pH > 8.7). The effect of pH solution on ciprofloxacin removal was examined in the range from 2.0 to 9.5 (Fig. 5). The ciprofloxacin adsorption yield increases with increasing pH solution for both initial concentrations of 5.0 and 10.0 mg L^{-1}. The maximal removal yields observed were 68% and 51% at pH values of 5.5 and 5.7 for initial concentrations of 5.0 and 10.0 mg L^{-1}, respectively. In contrast, the ciprofloxacin adsorption decreases when pH increases from 6.0 to 9.5, due to the electrostatic repulsion between the negatively charged chitosan (pH solution exceed pH_{Pzc}), and ciprofloxacin molecules [23,24], Also, the ciprofloxacin molecules is attracted by the alkaline solvent as pH solution increases.

3.5. Effect of contact time on ciprofloxacin adsorption

The contact time adsorption is an important parameter in equilibrium studies, also it provides valuable information about the mechanism of adsorption and the kinetic determining step in the process. Fig. 6 shows respectively the adsorption yield and capacity for ciprofloxacin removal on Al_2O_3@SiO_2-chitosan. The experimental data shows that the uptake of the ciprofloxacin was very fast in the first 30 min, however, after that, the amount of ciprofloxacin adsorbed remaining approximately constant and equilibrium time was reached in about 60 min [25,26]. The half adsorption times for ciprofloxacin removal on Al_2O_3@SiO_2-chitosan was less than 10 min. The adsorption kinetic was very fast, suggesting that the rate determining step might be the apparent chemical adsorption.

3.6. Kinetic modeling of ciprofloxacin adsorption

In order to analyze kinetic data for ciprofloxacin adsorption on Al_2O_3@SiO_2-chitosan, some of the commonly empirical models were applied. Pseudo-first-order, pseudo-second-order and intraparticle diffusion model was applied to determine the rate limiting step.

The kinetic models were adjusted to the experimental data, using the following equations [8]:

$$q_t = q_e\left(1-\exp^{-k_1 t}\right) \quad (3)$$

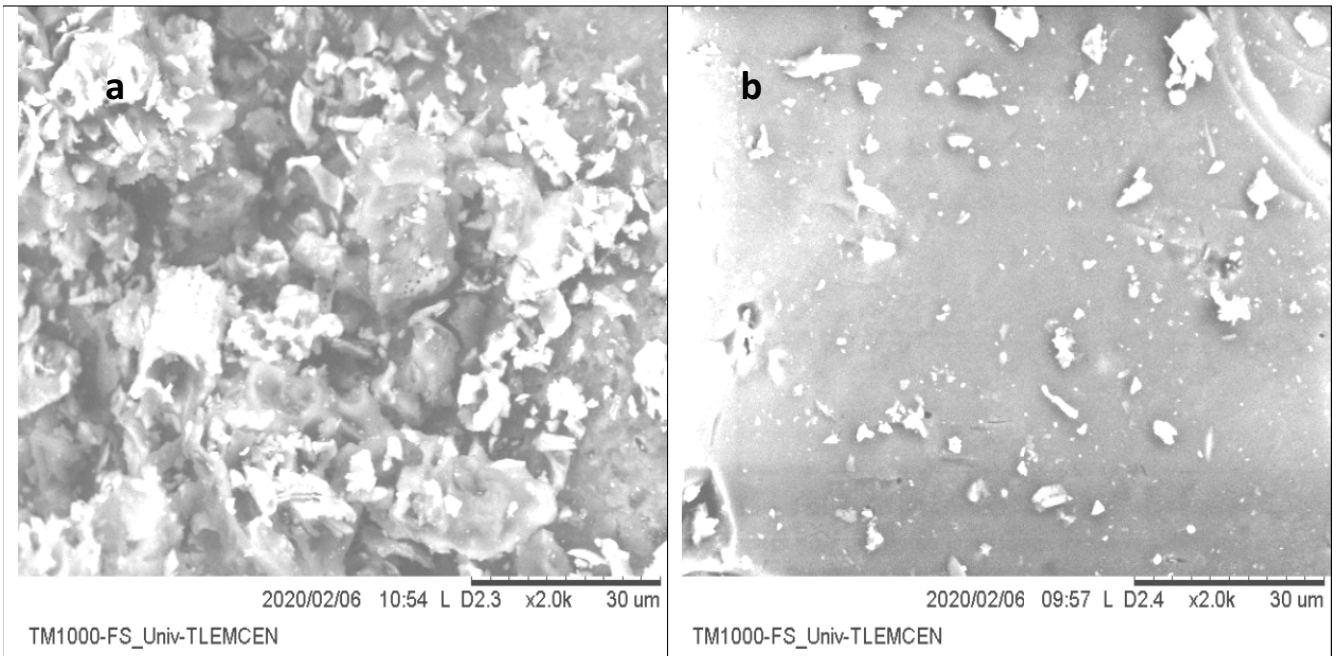

Fig. 4. SEM micrographs of Al_2O_3@SiO_2-chitosan microstructure before (a) and after (b) ciprofloxacin adsorption.

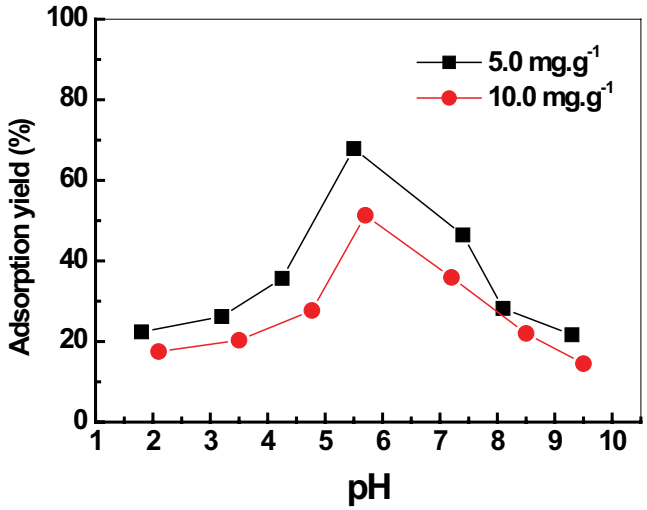

Fig. 5. Effect of pH solution value on the adsorption yield of ciprofloxacin on Al_2O_3@SiO_2-chitosan at room temperature; W = 0.010 g; V_{sol} = 30 mL; agitation speed = 250 rpm.

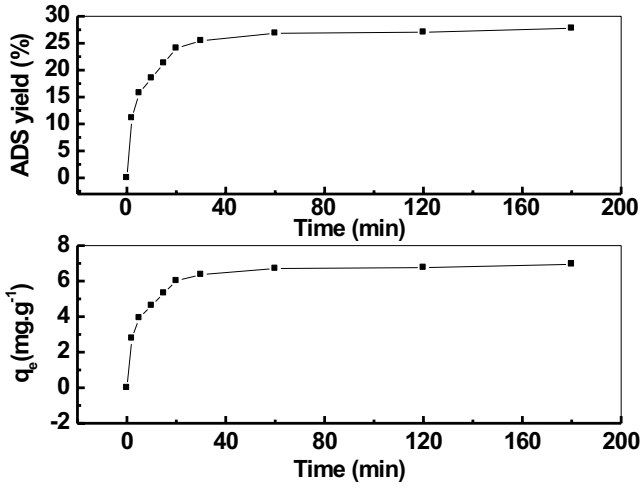

Fig. 6. Effect of contact time on ciprofloxacin adsorption onto Al_2O_3@SiO_2-chitosan; ciprofloxacin concentration = 10.0 mg L^{-1}; W_{ads} = 0.010 g; V_{sol} = 30 mL; agitation speed = 250 rpm.

where k_1 (min^{-1}) is the rate constant of the pseudo-first-order adsorption, q_t and q_e are the amount of ciprofloxacin adsorbed (mg g^{-1}) at time t and equilibrium time, respectively.

The pseudo-second-order adsorption kinetic rate equation is [27]:

$$q_t = \frac{k_2 q_e^2 t}{1 + k_2 q_e t} \tag{4}$$

where k_2 (g mg^{-1} min^{-1}) is the rate constant of the pseudo-second-order adsorption.

The intraparticle diffusion model can determine the possibility of intraparticle diffusion resistance that may affect the adsorption process of the pharmaceutical molecules. The intraparticle diffusion rate model is obtained by the following equation [28]:

$$q_t = k_i \cdot t_{1/2} + C \tag{5}$$

where k_i (intraparticle diffusion rate constant), and C is the constant rate equation.

The kinetic parameters and the linear correlation coefficient are listed in Table 1. The experimental data

Table 1
Kinetic modelling of ciprofloxacin adsorption onto Al_2O_3@SiO_2-chitosan

Ciprofloxacin	Parameters	Value
Pseudo-first-order	$q_{(cal)}$	3.51
	$q_{(exp)}$	6.94
	k_1 (min^{-1})	0.0495
	R	0.969
Pseudo-second-order	$q_{(cal)}$	7.19
	$q_{(exp)}$	6.94
	k_2 (g mg^{-1} min^{-1})	0.0323
	R	0.999
Intraparticle diffusion	$q_{(cal)}$	8.31
	$q_{(exp)}$	6.94
	k_{ID} (min^{-1})	0.415
	R	0.801
	C	2.75

(Table 1) are highly correlated (R > 0.99) and it successfully fitted by the pseudo-second-order models (Fig. 7), in which all calculated parameters were more adequate with experimental values [29]. The results show also, that intraparticle diffusion modeling for ciprofloxacin adsorption onto Al_2O_3@SiO_2-chitosan shows a high deviation between experimental data and the theoretical intraparticle model (Table 1). This result is in agreement with the above kinetic study leads to very fast adsorption process, limiting by chemical interaction of ciprofloxacin molecules with functional groups of Al_2O_3@SiO_2-chitosan [30,31].

3.7. Adsorption equilibrium of ciprofloxacin

Experimental adsorption isotherm data of ciprofloxacin onto Al_2O_3@SiO_2-chitosan are shown in Fig. 8. Adsorption equilibrium gives an indication about the maximum adsorption capacity for the ciprofloxacin at certain operating conditions. It also allows identifying the nature of adsorption process; physical or chemical, and it gives insight into surface properties of adsorbent [31]. In order to study the effect of initial ciprofloxacin concentration on the adsorption capacity onto Al_2O_3@SiO_2-chitosan, several experiments were also undertaken by varying the initial ciprofloxacin concentration from the range 10 to 100 mg L^{-1}, with fixed mass of Al_2O_3@SiO_2-chitosan (0.010 g). It can see clearly, that the adsorption capacity increases with increasing initial ciprofloxacin concentration. The maximal adsorption capacity was 31 mg g^{-1}. We suggest that Al_2O_3@SiO_2-chitosan is an effective adsorbent in separation and pre-concentration of ciprofloxacin from aqueous solution. Langmuir and Freundlich isothermal models were employed to evaluate the obtained experimental data [32,33]. The Langmuir model is suitable for monolayer adsorption onto available surface, and expressed by the following equation:

$$q_e = \frac{q_m K_L C_e}{1 + K_L C_e} \quad (6)$$

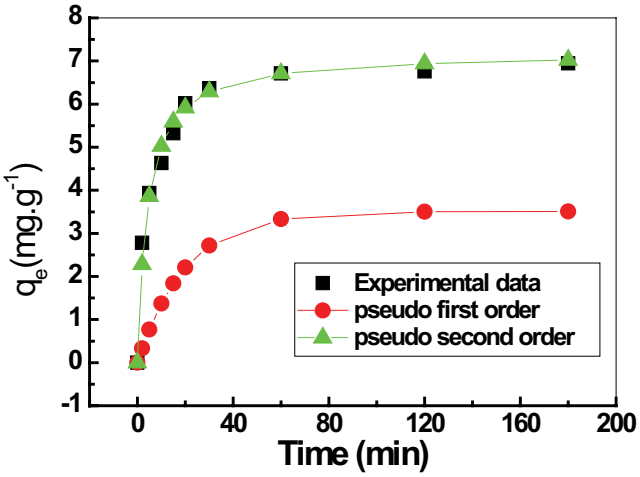

Fig. 7. Kinetic modelling of ciprofloxacin adsorption onto Al_2O_3@SiO_2-chitosan; ciprofloxacin concentration = 10.0 mg L^{-1}; W_{ads} = 0.010 g; V_{sol} = 30 mL; agitation speed = 250 rpm.

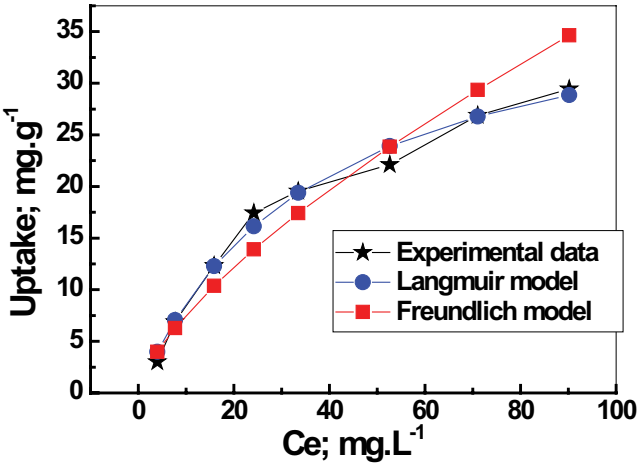

Fig. 8. Adsorption isotherm modelling of ciprofloxacin onto Al_2O_3@SiO_2-chitosan, at room temperature; W_{ads} = 0.010 g; V_{sol} = 30 mL; agitation speed = 250 rpm.

The Freundlich model is an empirical equation used to describe heterogeneous adsorption systems, can be represented as follows:

$$q_e = K_F \cdot C_e^{1/n} \quad (7)$$

where C_e is the equilibrium concentration of ciprofloxacin (mg L^{-1}), q_e the amount of ciprofloxacin adsorbed onto Al_2O_3@SiO_2-chitosan, K_L is the Langmuir adsorption constant (L mol^{-1}), q_{max} is the maximum amount of ciprofloxacin that can be adsorbed, K_F is the Freundlich adsorption constant and n is a constant which indicate the capacity and intensity of adsorption.

The Langmuir theoretical curve was found to be more adequate with the experimental data of ciprofloxacin adsorption (Table 2). The correlation coefficients were high (R = 0.99). The essential characteristic of Langmuir isotherm

Table 2
Freundlich and Langmuir model constants for ciprofloxacin adsorption onto Al_2O_3@SiO_2-chitosan

Models	Parameters	Ciprofloxacin
Langmuir model	K_L	0.0273
	q_m	40.58
	R_L	0.268
	R	0.99
Freundlich model	K_F	1.52
	n	1.44
	R	0.97

can be described by a separation factor, which is defined by the following equation:

$$R_L = \frac{1}{1 + k_L \cdot C_e} \tag{8}$$

The value of R_L indicates the nature of Langmuir isotherm, it is considered to be a favorable process when the value is within the range 0–1. So the calculated R_L values (0.268), indicates a favorable adsorption process, and we suggest a monolayer adsorption of ciprofloxacin onto Al_2O_3@SiO_2-chitosan. Multilayer adsorption from solution is highly uncommon compared than from the gas phase, because of the stronger screening interaction forces in condensed fluids [34,35].

3.8. Effect of temperature and thermodynamic study

In environmental engineering practice, both energy and entropy factors must be considered in order to determine which process will occur spontaneously. The Gibbs free energy change, ΔG is the fundamental criterion of spontaneity. The apparent thermodynamic parameters ΔH and ΔS for ciprofloxacin adsorption process were calculated from the slopes and intercepts of the linear variation of ($\ln K_d$) vs. ($1/T$) by the following expression [36].

$$\ln K_d = \frac{\Delta S}{R} - \frac{\Delta H}{RT} \tag{9}$$

The apparent free energy (ΔG) for ciprofloxacin adsorption was calculated by Eq. (10):

$$\Delta G = \Delta H - T\Delta S \tag{10}$$

Further, the thermodynamic equilibrium constant, K_d [Eq. (11)], obtained from the ciprofloxacin distribution between bulk solution and adsorbent surface, was used to compute the apparent thermodynamic parameters [37–39]:

$$K_d = \frac{(C_0 - C_e)V}{C_e m} \tag{11}$$

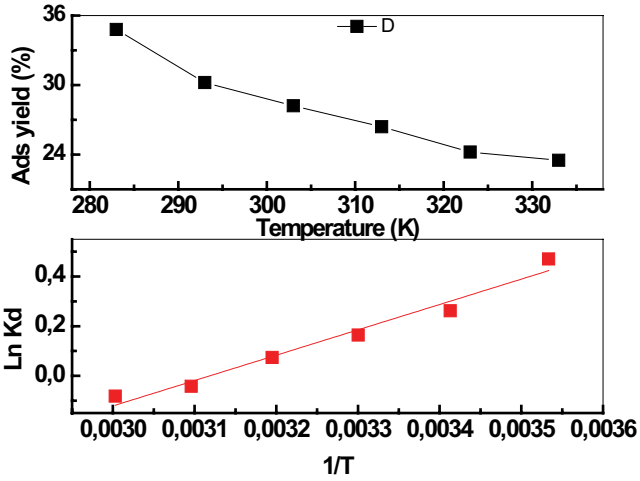

Fig. 9. Plot of ($\ln K_d$) vs. ($1/T$) on ciprofloxacin adsorption onto Al_2O_3@SiO_2-chitosan; initial ciprofloxacin concentration = 10.0 mg L^{-1}; W_{ads} = 0.010 g; V_{sol} = 30 mL; agitation speed = 250 rpm.

The calculated apparent thermodynamic parameters for ciprofloxacin adsorption are summarized in Table 3.

The negative values of ΔG indicate a spontaneous ciprofloxacin adsorption process, with high affinity towards Al_2O_3@SiO_2-chitosan surface. However, the negative values of ΔH, confirm an exothermic adsorption process (Fig. 9). The negative value of ΔS reflects the decrease in randomness at the solid–liquid interface of Al_2O_3@SiO_2-chitosan, suggesting the presence of significant changes in the external surface of adsorbent [40].

4. Conclusion

A green polymeric matrix Al_2O_3@SiO_2-chitosan was investigated for ciprofloxacin adsorption. Several parameters examined in this work, including contact time effect, pH solution effect, the concentration of ciprofloxacin, and temperature. The results show that Al_2O_3@SiO_2-chitosan exhibit, fast kinetic and potential adsorption capacity towards ciprofloxacin, around 31 mg g^{-1}, in one adsorption cycle. The optimum pH solution for ciprofloxacin adsorption ranges from 5.0 to 5.5.

Table 3
Thermodynamics parameters for ciprofloxacin adsorption onto Al_2O_3@SiO_2-chitosan

Ciprofloxacin	ΔH, (kJ mol^{-1})	ΔS, (J mol^{-1} K^{-1})	ΔG (kJ mol^{-1})				
R = 0.986	–08.49	–26.49	283 K	293 K	303 K	313 K	323 K
			–1.001	–0.728	–0.463	–0.198	–0.066

SEM micrographs analysis reveals the presence of cavities and different morphological and irregular shape. These micrographs also, noticed that the available surface of Al_2O_3@SiO_2-chitosan was influenced by ciprofloxacin after adsorption. FTIR spectroscopy characterization confirms that chitosan was successfully cross-linked onto Al_2O_3@SiO_2 surface. The negative value of Gibbs free energy (ΔG) indicates the spontaneous nature of ciprofloxacin adsorption. According to the simple synthesis approach, environmental friendliness, and adsorption efficiency, Al_2O_3@SiO_2-chitosan could be a perfect alternative adsorbent for removal and uptake of ciprofloxacin from the aqueous medium.

References

[1] R.E. Hester, R.M. Harrison, Pharmaceuticals in the Environment, Royal Society of Chemistry, 2015.

[2] Z. Feng, K. Odelius, G.K. Rajarao, M. Hakkarainen, Microwave carbonized cellulose for trace pharmaceutical adsorption, Chem. Eng. J., 34 (2018) 557–566.

[3] S.C. Kollarahithlu, R.M. Balakrishnan, Adsorption of ibuprofen using cysteine-modified silane-coated magnetic nanomaterial, Environ. Sci. Pollut. Res., 26 (2019) 34117–34126.

[4] Q. Sui, X. Cao, S. Lu, W. Zhao, Z. Qiu, G. Yu, Occurrence, sources and fate of pharmaceuticals and personal care products in the groundwater: a review, Emerg. Contam., 1 (2015) 14–24.

[5] M. Huerta-Fontela, M.T. Galceran, F. Ventura, Occurrence and removal of pharmaceuticals and hormones through drinking water treatment, Water Res., 45 (2011) 1432–1442.

[6] J.W. Hounfodji, W.G. Kanhounnon, G. Kpotin, G.S. Atohoun, J. Lainé, Y. Foucaud, M. Badawi, Molecular insights on the adsorption of some pharmaceutical residues from wastewater on kaolinite surfaces, Chem. Eng. J., 407 (2021) 127176, doi: 10.1016/j.cej.2020.127176.

[7] A. Yessoufou, D. Mama, F. Suanon, E.A. Alamou, B. Fayomi, C. Degbey, C.A. Dedjiho, Pharmaceuticals and personal care products (PPSPS) in the aquatic environment: status and issues in the Republic of Benin, Res. J. Pharm. Sci., 5 (2016) 1–15.

[8] G. Wernke, Q.L. Shimabuku-Biadola, T.R.T. Dos Santos, M.F. Silva, M.R. Fagundes-Klen, R. Bergamasco, Adsorption of cephalexin in aqueous media by graphene oxide: kinetics, isotherm, and thermodynamics, Environ. Sci. Pollut. Res., 27 (2020) 4725–4736.

[9] B.I. Escher, R. Baumgartner, M. Koller, K. Treyer, J. Lienert, C.S. McArdell, Environmental toxicology and risk assessment of pharmaceuticals from hospital wastewater, Water Res., 45 (2011) 75–92.

[10] A. Gómez-Avilés, L. Sellaoui, M. Badawi, A. Bonilla-Petriciolet, J. Bedia, C. Belver, Simultaneous adsorption of acetaminophen, diclofenac and tetracycline by organo-sepiolite: experiments and statistical physics modelling, Chem. Eng. J., 404 (2021) 126601, doi: 10.1016/j.cej.2020.126601.

[11] V. Jarlier, Role of cross-transmission in resistance to antibiotics: control procedures in French hospitals, Bull. de l Acad. Natl. de Med., 203 (2019) 170–178.

[12] M.D. Vedenyapina, A.Y. Kurmysheva, A.K. Rakishev, Y.G. Kryazhev, Activated carbon as sorbents for treatment of pharmaceutical wastewater, Solid Fuel Chem., 53 (2019) 382–394.

[13] D. Simazaki, R. Kubota, T. Suzuki, M. Akiba, T. Nishimura, S. Kunikane, Occurrence of selected pharmaceuticals at drinking water purification plants in Japan and implications for human health, Water Res., 76 (2015) 187–200.

[14] T. Akar, A.S. Ozcan, S. Tunali, A. Ozcan, Biosorption of a textile dye (Acid blue 40) by cone biomass of *Thuja orientalis*: estimation of equilibrium, thermodynamic and kinetic parameters, Bioresour. Technol., 99 (2008) 3057–3065.

[15] R. Herrero, P. Lodeiro, R. Rojo, A. Ciorba, P. Rodríguez, M.E.S. Vicente, The efficiency of the red alga *Mastocarpus stellatus* for remediation of cadmium pollution, Bioresour. Technol., 99 (2008) 4138–4146.

[16] D.J. Ju, I.G. Byun, J.J. Park, C.H. Lee, G.H. Ahn, T.J. Park, Biosorption of a reactive dye (Rhodamine-B) from an aqueous solution using dried biomass of activated sludge, Bioresour. Technol., 99 (2008) 7971–7975.

[17] J. de Jesus Menk, A.I.S. do Nascimento, F.G. Leite, R.A. de Oliveira, A.F. Jozala, J.M. de Oliveira Junior, D. Grotto, Biosorption of pharmaceutical products by mushroom stem waste, Chemosphere, 237 (2019) 124515, doi: 10.1016/j.chemosphere.2019.124515.

[18] J.R. Xavier, Electrochemical and dynamic mechanical studies of newly synthesized polyurethane/SiO_2-Al_2O_3 mixed oxide nanocomposite coated steel immersed in 3.5% NaCl solution, Surf. Interfaces, 22 (2021) 100848, doi: 10.1016/j.surfin.2020.100848.

[19] N. Ferrah, Comparative study of mercury(II) species removal onto naked and modified magnetic chitosan flakes coated ethylenediaminetetraacetic-disodium: kinetic and thermodynamic modeling, Environ. Sci. Pollut. Res., 25 (2018) 24923–24938.

[20] R.J. Kalbasi, M. Kolahdoozan, S.M. Vanani, Preparation, characterization and catalyst application of ternary interpenetrating networks of poly 4-methyl vinyl pyridinium hydroxide–SiO_2–Al_2O_3, J. Solid State Chem., 184 (2011) 2009–2016.

[21] Y.D. Lamidi, S.S. Owoeye, S.M. Abegunde, Preparation and characterization of synthetic tobermorite (CaO–Al_2O_3–SiO_2–H_2O) using bio and municipal solid wastes as precursors by solid state reaction, Boletín de la Sociedad Española de Cerámica y Vidrio, 61 (2022) 76–81.

[22] J. Meng, C. Li, X. Chen, C. Song, C. Liang, Seed-assisted synthesis of ZSM-48 zeolite with low SiO_2/Al_2O_3 ratio for n-hexadecane hydroisomerization, Microporous Mesoporous Mater., 309 (2020) 110565, doi: 10.1016/j.micromeso.2020.110565.

[23] M. Shafaati, M. Miralinaghi, R.H.S.M. Shirazi, E. Moniri, The use of chitosan/Fe_3O_4 grafted graphene oxide for effective adsorption of rifampicin from water samples, Res. Chem. Intermed., 46 (2020) 5231–5254.

[24] L. Laysandra, I.J. Ondang, Y.H. Ju, B.H. Ariandini, A. Mariska, F.E. Soetaredjo, S. Ismadji, Highly adsorptive chitosan/saponin-bentonite composite film for removal of methyl orange and Cr(VI), Environ. Sci. Pollut. Res., 26 (2019) 5020–5037.

[25] N.S. Awwad, H.M.H. Gad, M.I. Ahmad, H.F. Aly, Sorption of lanthanum and erbium from aqueous solution by activated carbon prepared from rice husk, Colloids Surf., B, 81 (2010) 593–599.

[26] H. Li, D.L. Xiao, H. He, R. Lin, P.L. Zuo, Adsorption behavior and adsorption mechanism of Cu(II) ions on amino-functionalized magnetic nanoparticles, Trans. Nonferrous Met. Soc. China, 23 (2013) 2657–2665.

[27] L. Lin, W. Jiang, P. Xu, Comparative study on pharmaceuticals adsorption in reclaimed water desalination concentrate using biochar: impact of salts and organic matter, Sci. Total Environ., 601 (2017) 857–864.

[28] A.E. Ofomaja, E.B. Naidoo, A. Pholosi, Intraparticle diffusion of Cr(VI) through biomass and magnetite coated biomass: a comparative kinetic and diffusion study, S. Afr. J. Chem. Eng., 32 (2020) 39–55.

[29] P. Moeini, A. Bagheri, Adsorption kinetic modeling of toxic vapors on activated carbon in the batch reactor, Res. Chem. Intermed., 46 (2020) 5547–5566.

[30] G. Venkatesan, V. Rajagopalan, Adsorption kinetic models for the removal of Cu(II) from aqueous solution by clay liners in landfills, Int. J. Environ. Sci. Technol., 13 (2016) 1123–1130.

[31] Y.M. Magdy, H. Altaher, E. El-Qada, Removal of three nitrophenols from aqueous solutions by adsorption onto char ash: equilibrium and kinetic modeling, Appl. Water Sci., 8 (2018) 1–15.

[32] Y. Tang, L. Che, X. We, Q. Ya, T. Li, Removal of lead ions from aqueous solution by the dried aquatic plant, *Lemna perpusilla Torr*, J. Hazard. Mater., 244–245 (2013) 603–612.

[33] Y. Tan, M. Chen, Y. Hao, High efficient removal of Pb(II) by amino-functionalized Fe_3O_4 magnetic nano-particles, Chem. Eng. J., 191 (2012) 104–111.
[34] F.B. Scheufele, A.N. Módenes, C.E. Borba, C. Ribeiro, F.R. Espinoza-Quiñones, R. Bergamasco, N.C. Pereira, Monolayer–multilayer adsorption phenomenological model: kinetics, equilibrium and thermodynamics, Chem. Eng. J., 284 (2016) 1328–1341.
[35] N. Ferrah, D. Merghache, S. Meftah, Benbellil, A new alternative of a green polymeric matrix chitosan/alginate-polyethyleniminemethylene phosphonic acid for pharmaceutical residues adsorption, Environ. Sci. Pollut. Res., 29 (2022) 13675–13687.
[36] F. Gode, E. Pehlivan, A comparative study of two chelating ion-exchange resins for the removal of chromium(III) from aqueous solution, J. Hazard. Mater. B, 100 (2003) 231–243.
[37] A. Gotzias, E. Kouvelos, A. Sapalidis, Computing the temperature dependence of adsorption selectivity in porous solids, Surf. Coatings Technol., 350 (2018) 95–100.
[38] A. Gotzias, Calculating adsorption isotherms using Lennard Jones particle density distributions, J. Phys.: Condens. Matter, 31 (2019) 435901, doi: 10.1088/1361-648X/ab2c94.
[39] A. Gotzias, A. Sapalidis, E. Favvas, Hydrogen adsorption simulations in isomorphous borohydride and imidazolate frameworks: evaluations using interpolation, Int. J. Hydrogen Energy, 46 (2021) 19778–19787.
[40] H. Guo, Y. Ren, X. Sun, Y. Xu, X. Li, T. Zhang, J. Kang, D. Liu, Removal of Pb^{2+} from aqueous solutions by a high-efficiency resin, Appl. Surf. Sci., 283 (2013) 660–667.